

Radiative and nonradiative processes in the optical cycle of the F_3^+ center in LiF

G. Baldacchini, M. Cremona,* G. d'Auria, R. M. Montereali, and V. Kalinov†

ENEA, Dipartimento Innovazione, Settore Fisica Applicata, Centro Ricerche Frascati, Casella Postale 65, 00044 Frascati, Rome, Italy

(Received 29 February 1996; revised manuscript received 16 July 1996)

Lithium fluoride stands apart from the other alkali halide crystals because of its good physical properties and the excellent thermal stability of the color centers. Among them the F_3^+ after absorbing at ~ 450 nm emits at ~ 535 nm, with an unusual dependence on time, excitation power, and temperature. Accurate optical measurements as a function of temperature have confirmed the existence of a triplet state, which acts as a trap for a sizable fraction of the excited F_3^+ centers. In addition, the singlet and triplet states are connected by nonradiative transitions involving multiphonon processes, which have been crucial in assessing the energy position of the ground triplet state ~ 1 eV below the relaxed excited singlet state. [S0163-1829(96)00148-8]

I. INTRODUCTION

Alkali halide crystals with color centers have been at the center of attention of the solid-state community since the beginning of this century and, besides a direct interest in their peculiar optical properties, they have been widely utilized as prototype cases for more complex point defects in crystals.¹ In more recent times they have been actively studied experimentally and theoretically to clarify fundamental processes of radiative and nonradiative transitions,² and moreover they came to be well known as a suitable optical material for tunable solid-state lasers from the visible to the near-infrared spectral region.³ Among such crystals, lithium fluoride occupies a special place because it can host point defects that emit efficiently even at room temperature and it is not hygroscopic, unlike the other salts. Studies on LiF-based lasers have established that lasing at room temperature (RT) and in the pulsed regime is possible in the spectral ranges $0.65\text{--}0.74\ \mu\text{m}$ (F_2 centers), $0.84\text{--}1.12\ \mu\text{m}$ (F_2^- centers), $1.09\text{--}1.26\ \mu\text{m}$ (F_2^- centers), and $0.51\text{--}0.57\ \mu\text{m}$ (F_3^+ centers),⁴⁻⁷ although these centers suffer from bleaching effects with the exception of the F_2^- centers. Some interesting applications, such as the generation of optical phase conjugation waves, have been implemented using the nonlinear optical behavior of LiF crystals containing mainly F_3^+ centers.^{8,9}

In spite of the rich and still promising field of applied research, basic knowledge of the optical properties of most of the color centers in LiF is still lagging behind. First of all, the F center, which is commonly associated with the absorption band at ~ 250 nm, has not yet produced any emission, although a little luminescence is theoretically expected.^{10,11} However, such emission would be difficult to observe as, according to the hydrogenoid model of the F center imbedded in a dielectric medium,¹² it should appear at ~ 900 nm. This is the region where F_2^+ center luminescence is emitted, and it is impossible to produce samples without at least a few of these centers, which besides their fundamental band at ~ 630 nm also absorb at ~ 250 nm. Second, it is not possible to color LiF additively; it can only be colored by various irradiation techniques that produce both F and more complex centers. These centers are often transformed one into another under either pumping or thermal cycles, or under both, and

the absorption and emission bands of different centers may overlap each other, as is the case for the F_2 and F_3^+ centers. It is well known that the excitation of the absorption band at ~ 450 nm of a colored LiF crystal produces two emissions; a green one peaked at ~ 535 nm, and a red one at ~ 670 nm. Optical investigations and polarization measurements have shown that the defects responsible for the green and red emissions are the F_3^+ and F_2 centers, respectively.¹³ At RT the F_3^+ absorption band has a maximum at ~ 458 nm and almost coincides with the F_2 absorption band, whose maximum is at ~ 441 nm. The overlapping of the two absorption bands allows simultaneous lasing in the pulsed regime in the green and red spectral regions.¹⁴⁻¹⁶ However, such a coincidence also causes serious difficulties in the preparation of active media with low losses at the pumping wavelengths ($400\text{--}490$ nm) and in the laser oscillation of the F_3^+ color center ($510\text{--}570$ nm). Moreover, investigation of the optical properties of F_3^+ centers is prevented by the presence of F_2 centers, which are inevitably produced by bombardment with ionizing radiation. More F_2 centers are created at room temperature than at liquid-nitrogen¹⁴ (LNT) and dry-ice temperature,^{15,16} and a further decrease in their number can be obtained by pumping the colored crystal with excimer laser radiation at 308 nm,¹⁶ which falls within the second absorption band of F centers.^{17,18}

The present paper is devoted to an accurate study of the optical cycle of the F_3^+ center in crystals containing, as far as possible, just this center. Only in such extreme conditions is it possible to definitely confirm the existence and determine exactly the properties of a triplet state,¹⁴ which has been invoked to explain a surprising emission intensity quenching at ~ 535 nm under strong optical pumping of the absorption band at ~ 450 nm. This same decreasing of the emission intensity has also been ascribed to a reduction of luminescence quantum yield with temperature,¹⁹ and to a complex photochemical process involving both F_2 and F_3^+ centers.^{20,21} It is of the utmost importance to carry out further experiments with well characterized crystals, concerning various color centers, in which the temperature is well controlled. The work done for these purposes has been organized as in the following. In Sec. II the preparation of the LiF crystal and the experimental apparatus is described in detail, while the most significant experimental results are

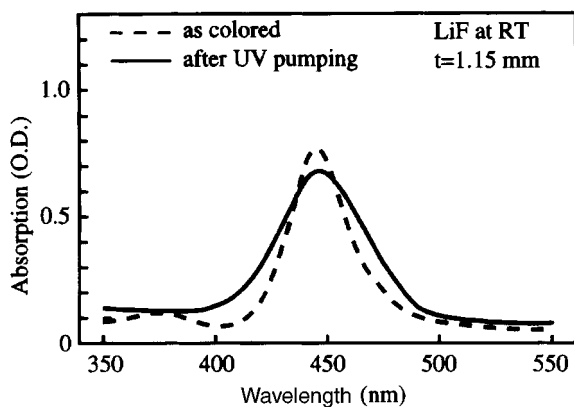


FIG. 1. Absorption spectrum at RT of a γ -irradiated LiF crystal before (dashed line) and after (solid line) excimer laser pumping.

presented in Sec. III. The optical cycle and the rate equations with a few significant solutions pertinent to the results of this work are discussed in Sec. IV. Data relative to the theoretical model are discussed in Sec. V, followed by conclusions in Sec. VI.

II. EXPERIMENTAL PROCEDURES

LiF crystals containing impurity ions at less than 10 ppm were colored with γ rays from a ^{60}Co source at dry-ice temperature. The samples used in the experiments measured $\sim 20 \times 40 \times 1.15 \text{ mm}^3$; they were subjected to an exposure rate of 0.7 kC/kg h (equivalent to $2.78 \times 10^6 \text{ R/h}$) and an irradiation dose of 7 kC/kg. After irradiation the crystals contained mainly F , F_2 , F_3 , and F_3^+ centers. Figure 1 shows a portion of the absorption spectrum (dashed line) of one such crystal containing F_2 (more) and F_3^+ (fewer) centers absorbing at 445 nm and F_3 centers absorbing at 375 nm. The F band, not shown in Fig. 1, had an absorption of ~ 10 optical density. By pumping the crystal with the 308-nm line of an excimer laser at RT, the F_2 centers were destroyed and transformed into F_3^+ centers, as clearly shown by the corresponding absorption spectrum (solid line): the much wider absorption band and the peak slightly shifted toward longer wavelengths indicate a predominance of F_3^+ centers.^{15,18} This transformation can be seen with the naked eye, since it is accompanied by the crystal changing from yellow after coloration to a greenish shade following UV exposure. However, a final check was made by means of emission measurements, exciting the samples with the 457-nm line of an Ar^+ laser. Figure 2 shows the luminescence spectra at RT taken before (dashed line) and after (solid line) UV exposure. The F_3^+ band emission increases with respect to and at the expense of the F_2 band emission after exposure.

A sample containing a majority of F_3^+ centers and a lot of F centers was prepared using the above procedure and studied experimentally. Emission measurements were taken in both collinear and perpendicular geometries of the pumping source and the detector, with the sample placed in a variable-temperature cryostat. The 457-nm line of an Ar^+ laser was used to excite the F_3^+ color centers, and a photomultiplier with S20 response monitored the emission filtered by a 25-cm focal length monochromator. The pumping light was modulated by a chopper and the signal analyzed by the

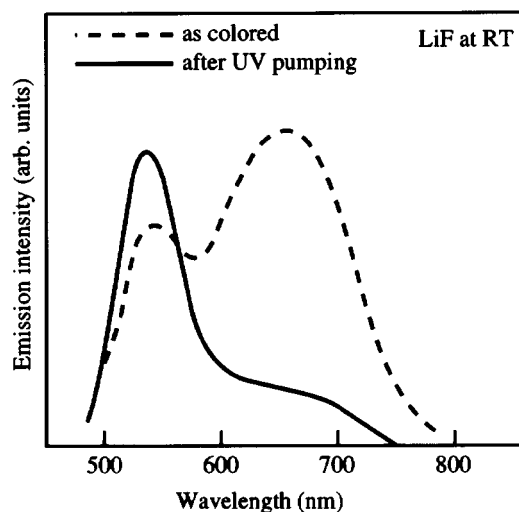


FIG. 2. Emission spectrum at RT of a γ -irradiated LiF crystal before (dashed line) and after (solid line) excimer laser pumping obtained by excitation with the 457-nm line of an Ar^+ laser.

lock-in technique and acquired by an A/D system. A scanner was also used on the laser beam to study transient phenomena. In order to avoid any appreciable local heating the power of the pumping laser never exceeded 100 mW on the crystals, and the laser beam was not focused. Moreover the two big flat faces of the crystals were mounted tightly between two gold-plated copper pieces of the cold finger of the cryostat in order to assure a good thermal contact for dissipating the absorbed energy of the laser beam. Absorption spectra before and after each emission measurement were obtained by a Perkin Elmer $\lambda 19$ spectrophotometer. The absorption at a fixed wavelength of 460 nm under 457-nm laser pumping was monitored by using the filtered light from a tungsten lamp and the same experimental setup.

III. EXPERIMENTAL RESULTS

A marked decrease in luminescence accompanied by a slight color change from green to green-yellow were observed in the first few seconds of laser pumping. This remarkable phenomenon is reported quantitatively in Fig. 3, where the time evolution of the F_3^+ emission at 530 nm after switching on the 457-nm excitation is shown at RT and LNT. The initial intensity decays exponentially towards a steady-state value with constant pumping power. This behavior is similar, but with different time and intensity scales, for all the pumping powers and wavelengths within the F_3^+ emission band.²² In particular, the initial (transient) and the final (stationary) values of the emission intensity unambiguously show, respectively, a linear dependence and a saturation effect with pumping power. In the same conditions, the weak luminescence of the remaining F_2 centers, peaked at 670 nm, does not show any time evolution or saturation effects, which are evidently originated only by F_3^+ centers. Similar behavior was also observed in a LiF crystal colored at RT with a 30-keV electron beam.²³ Once the emission reaches the stationary value, it remains there as long as the laser pumping power is kept constant. However, a complete recovery of the luminescence is obtained when the pump laser

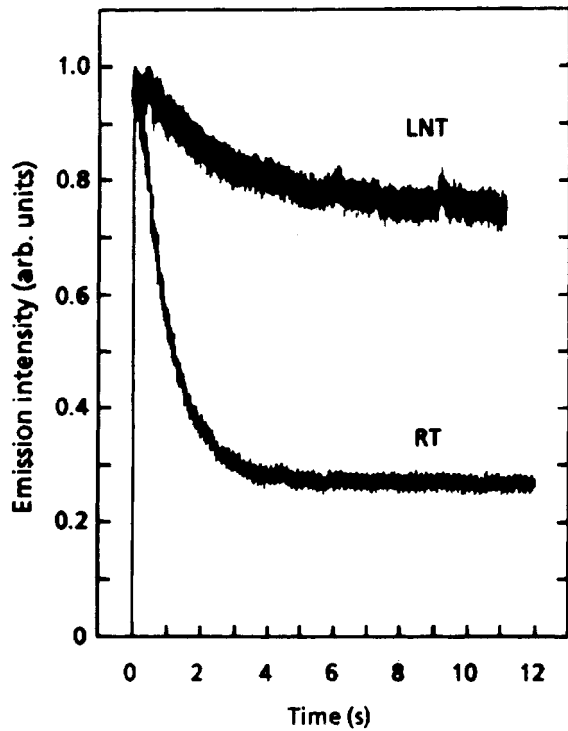


FIG. 3. Time evolution of the normalized emission at 530 nm after switching on the laser excitation at 457 nm with a power of 42.5 mW at RT and LNT.

is switched off long enough and on again. For a more complete picture of the phenomenon, the time evolution of the absorption peak after switching the laser exciting light on and off was also investigated. After switching on the laser, the sample absorption decreased to a different equilibrium value, and removal of the laser light resulted in a spontaneous recovery towards the initial value of the absorption, as

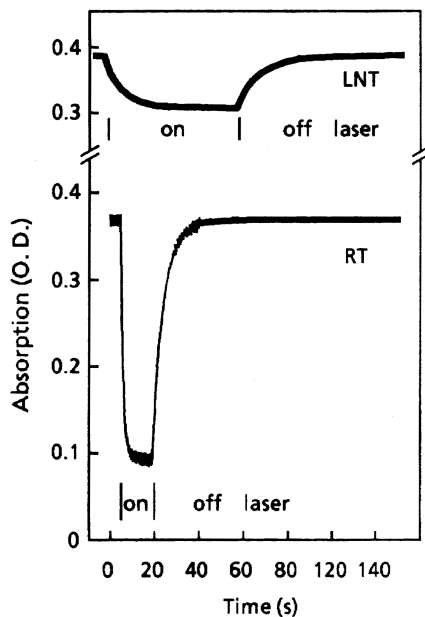


FIG. 4. Time evolution of the absorption at 460 nm after switching the laser excitation on and off at 457 nm with a power of 42.5 mW at RT and LNT.

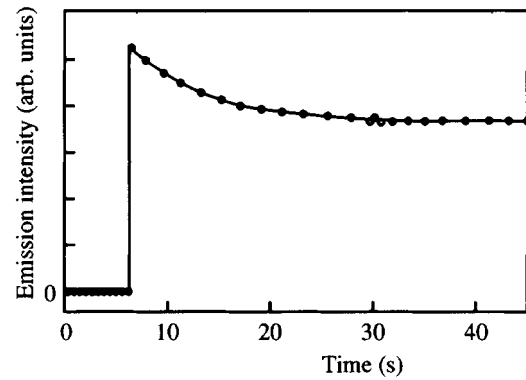


FIG. 5. Time dependence of the luminescence at LNT after switching on the pump laser (circles) and best fit with an exponential curve with a unique time constant $\tau_p = 7.20$ s (solid line).

shown in Fig. 4, both at RT and LNT.

The time behavior of the signal variations in Figs. 3 and 4 can be described by exponential curves with a unique time constant τ_p (pumping) when the laser is switched on, and τ_r (recovery) when the laser is switched off. Figures 5 and 6 show two typical best fits to exponential functions of the experimental results at LNT and RT, respectively, and the agreement is very good. The time constant τ_p was then measured as a function of pumping power at different temperatures both in emission and in absorption experiments. Figure 7 reports τ_p vs pumping intensity at RT and LNT, as taken from absorption signals. Similar values were also obtained from luminescence signals. The time constant τ_r does not depend on the pumping power; its dependence on the temperature is reported in Fig. 8, as derived from absorption signals.

IV. OPTICAL CYCLE AND RATE EQUATIONS

The experimental results in Sec. III indicate the existence of a long-lived state in the optical cycle of the F_3^+ center, capable of momentarily trapping the electronic excitation. In previous works^{14,24,25} it was suggested that this energy level could be a triplet state, and Fig. 9 shows the energy-level diagram. The F_3^+ center can be excited from the ground-state (GS) 1A_1 to the first excited state $^1E_1^*$ by optical pumping $U_0 \neq 0$. After a relaxation time of the order of ps, the

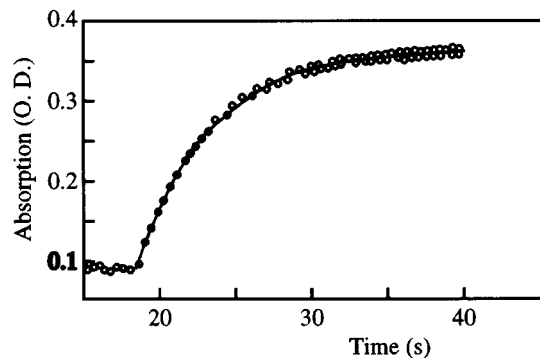


FIG. 6. Time dependence of the absorption at RT after switching off the pump laser (circles) and best fit with an exponential curve with a unique time constant $\tau_r = 4.86$ s (solid line).

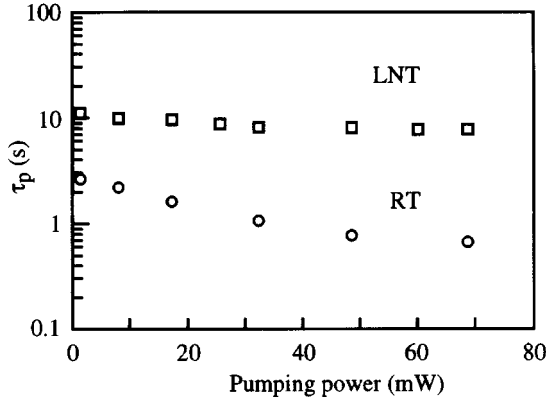


FIG. 7. Time constant τ_p as a function of pumping power at RT and LNT, measured from absorption.

excitation reaches the relaxed excited state (RES) 1E_1 , from where it can decay radiatively, with a time constant τ_0 , to the unrelaxed ground state (URGS) ${}^1A_1^*$, or reach, through a nonradiative transition and with probability W_1 , the ground triplet state (GTS) 3E_1 . From the triplet state the excitation can reach, through another nonradiative transition with probability W_2 , the unrelaxed ground-state ${}^1A_1^*$. From here the excitation eventually relaxes to the ground state in a time of the order of ps. Thus, the triplet state acts both as a trap for the excited population and as an efficient quenching of the emission. The possibility of an optical excitation to the higher-energy triplet state 3A_2 , which has recently received some attentions,^{26,27} has not been considered at this stage because it does not have relevant consequences on the present experimental and theoretical analysis, as it will be shown later on.

By considering that the lifetime τ_0 of the RES is of the order of a few ns (Refs. 28–33) and that the pump rate out of the GS, U_0 , could be $\sim 10^3 \text{ s}^{-1}$ at the maximum power used in the present experiments, it follows that only the GS, RES, and GTS states retain an appreciable population during the optical cycle. Therefore, by limiting the study to these three states, the optical cycle is described by the following rate equations:

$$\frac{dn_0}{dt} = -U_0 n_0 + \frac{1}{\tau_0} n_1 + W_2 n_2,$$

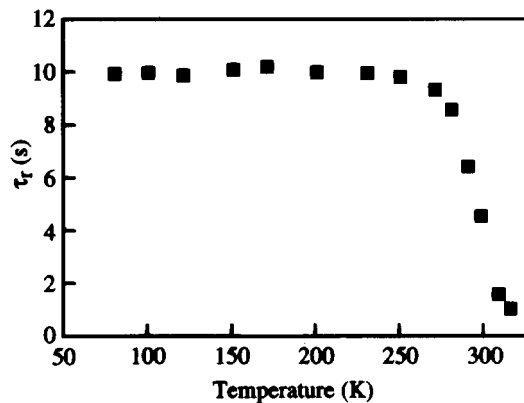


FIG. 8. Time constant τ_r as a function of temperature measured from absorption.

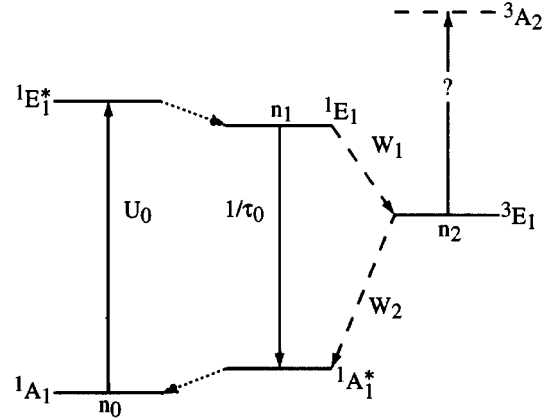


FIG. 9. Energy-level diagram of the F_3^+ center showing the radiative (—), nonradiative (-----), and relaxation transitions (·····).

$$\frac{dn_1}{dt} = +U_0 n_0 - \left(\frac{1}{\tau_0} + W_1 \right) n_1,$$

$$\frac{dn_2}{dt} = +W_1 n_1 - W_2 n_2,$$

$$N = n_0 + n_1 + n_2, \quad (1)$$

where N is the number of F_3^+ centers per cm^3 and the pump rate out of the GS is given by

$$U_0 = \sigma_0 \frac{I}{A h \nu}, \quad (2)$$

with $\sigma_0 = 7.1 \times 10^{17} \text{ cm}^2$ at $\lambda = 460 \text{ nm}$,³⁴ and where I is the pumping laser power, A the laser focusing area on the crystal, and $h\nu$ the energy of the laser photon. In the present experimental conditions, where the laser beam is not focused, $U_0 (\text{s}^{-1}) = 5260 \times I(\text{W})$, and, as the power never exceeds a few hundred mW, it is always $U_0 \tau_0 \ll 1$, which means that saturating conditions can be excluded. If it is also assumed that $\tau_0^{-1} \gg W_1, W_2$, as demonstrated later on, the temporal solutions of Eq. (1) to a sudden pumping excitation ($U_0 = 0$ for $t < 0$ and $U_0 \neq 0$ for $t \geq 0$), with the initial conditions given by $n_1(0) = n_2(0) = 0$, $n_0(0) = N$, are expressed as follows:

$$n_0(t) \cong N \frac{1}{1 + U_0 \tau_0 \frac{W_1}{W_2}} \left[1 + U_0 \tau_0 \frac{W_1}{W_2} e^{-t/\tau} \right],$$

$$n_1(t) \cong N U_0 \tau_0 \left[-e^{-t/\tau_0} + \frac{U_0 \tau_0 \frac{W_1}{W_2}}{1 + U_0 \tau_0 \frac{W_1}{W_2}} \right]$$

$$\times e^{-t/\tau} + \frac{1}{1 + U_0 \tau_0 \frac{W_1}{W_2}},$$

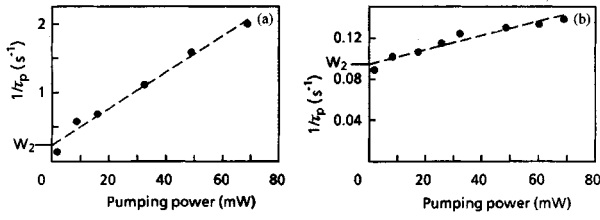


FIG. 10. Values of $(\tau_p)^{-1}$ as a function of pumping power at RT obtained from emission measurements (a) and at LNT from absorption measurements (b). The experimental data of $W_2 = (\tau_r)^{-1}$ are shown at $I=0$. The dashed line is the linear best fit.

$$n_2(t) \cong N \frac{U_0 \tau_0 \frac{W_1}{W_2}}{1 + U_0 \tau_0 \frac{W_1}{W_2}} [1 - e^{-t/\tau}], \quad (3)$$

where

$$\frac{1}{\tau} = (U_0 \tau_0 W_1 + W_2). \quad (4)$$

Thus, the populations of the three states are governed by a fast time τ_0 , which is the lifetime of the RES, and a much slower time τ , which coincides with the pumping time τ_p measured in the preceding kinetic experiments. Moreover, when the pumping intensity is switched off abruptly, the populations of the GS and GTS change exponentially, as clearly indicated by Eqs. (1), with a time constant W_2^{-1} that coincides with the recovery time τ_r .

From Eqs. (3) it is also possible to calculate the ratio between the initial and the final value of both the luminescence (see Fig. 3) and the absorption (see Fig. 4), which are given by the same expression:

$$\frac{n_1^{\max}}{n_1(\infty)} = \frac{n_0(0)}{n_0(\infty)} = 1 + U_0 \tau_0 \frac{W_1}{W_2}, \quad (5)$$

where n_1^{\max} is the maximum value of the population of the RES just after switching on the pumping laser, i.e., at least after $\sim 3\tau_0$.

V. DISCUSSION

The model of the F_3^+ center, represented schematically in Fig. 9, after some mathematical manipulations gives a few simple formulas that relate measurable quantities, such as the pumping time τ_p [Eq. (4)] and the absorption and emission

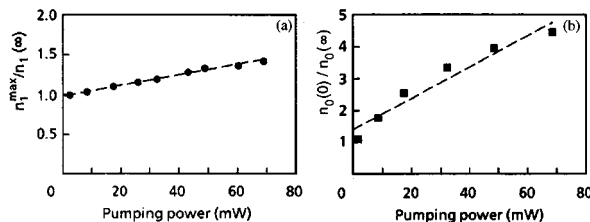


FIG. 11. Ratio of initial and final intensity of emission (a) and absorption (b) as a function of laser pump intensity at LNT and RT, respectively.

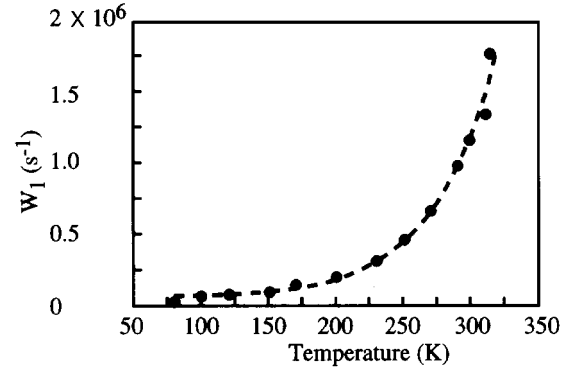


FIG. 12. Transition probability W_1 from the RES towards the GTS as a function of temperature. The dashed line is the best fit of the experimental data with Eq. (8).

signals [Eq. (5)], to the pump rate U_0 and to various intrinsic parameters of the optical cycle: τ_0 , W_1 , and W_2 . We can now verify the validity of the model in relation to the experimental results of Sec. III.

Figures 10(a) and 10(b) show the values of $(\tau_p)^{-1}$ as a function of pumping intensity, obtained at RT from the emission measurements and at LNT from the absorption measurements, respectively. A straight line fits the experimental points very well, as expected from Eq. (4). The intercept at $I=0$ coincides, as required by the model, with the value of $W_2 = (\tau_r)^{-1}$ as determined independently from absorption recovery time measurements.

Figures 11(a) and 11(b) show the ratio of the initial and final values of the F_3^+ luminescence and the F_3^+ absorption at LNT and RT, respectively, as a function of the pumping intensity. As expected from Eq. (5), there is a linear dependence with a unitary intercept for $I=0$.

The main experimental results for the F_3^+ centers are, therefore, fairly well explained by the present theory, which can be applied to calculate the values of W_1 from the measured values of $(\tau_p)^{-1}$ and $(\tau_r)^{-1}$ according to Eqs. (4) and (5), since the RES lifetime τ_0 is a known parameter. Figure 12 reports the value of W_1 thus obtained vs temperature by assuming $\tau_0=4$ ns, while Fig. 13 shows the values of $1/\tau_r = W_2$ as taken from Fig. 8. For the sake of completeness it is worthwhile to note that the value of W_1 , which is the nonradiative transition rate between the singlet state 1E_1 and

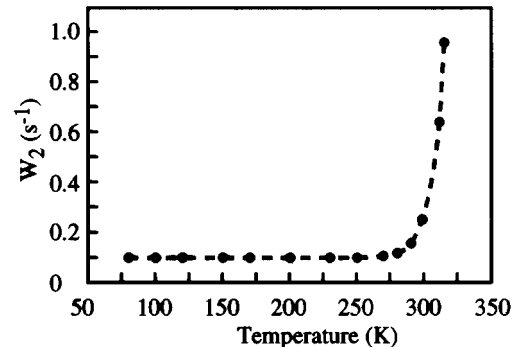


FIG. 13. Transition probability W_2 from the GTS towards the URGS as a function of temperature. The dashed line is the best fit of the experimental data with Eq. (8).

TABLE I. Parameters of Eq. (6) derived by fitting the experimental results of Figs. 12 and 13.

	$W_1(T)$	$W_2(T)$
h_s (s^{-1})	4.4×10^5	0.1
ΔE (meV)	2.3	1
h_m (s^{-1})	1.4×10^4	3×10^{-13}
$\hbar\omega$ (meV)	42.3	24.7
p	19	56

the triplet state 3E_1 , reported here in Fig. 12 at RT, coincides with the value obtained elsewhere independently with similar techniques and analysis;²⁷ this agreement represents a much welcome validation of the whole set of present results. Anyway it is evident that, above 200 K for W_1 and 275 K for W_2 , a multiphonon process is involved in both transitions. The whole behavior can be explained with a model for nonradiative transitions of impurities in insulating crystals^{35–37} that includes a spontaneous process and a stimulated one. The former involves the emission of a few phonons, while the latter is characterized by a multiphonon emission and dominates at high temperatures, where the average occupation number of phonons is higher. So the transition probabilities are described by the following expression:

$$W(T) = h_s e^{-\Delta E/kT} + h_m \left(\frac{1}{1 - e^{-\hbar\omega/kT}} \right)^p, \quad (6)$$

where ΔE is the activation energy for the spontaneous emission, $\hbar\omega$ is the energy of the phonon involved in the multiphonon assisted processes, and p is the number of phonons. A best fit of the experimental data with this formula is shown in Figs. 12 and 13 by dashed lines, and the parameters obtained are given in Table I. The values of the excitation energy ΔE are surprising small, especially for the transition probability W_2 , which below 250 K seems to require only a temperature-independent relaxation process. Anyway, leaving this interest subject to future and more detailed investigations, it is important to note that at high temperatures the multiphonon term in Eq. (6) takes over the relaxation processes. As a consequence, from the results of Table I it is possible to infer the energy separation of the GTS with respect to the RES and URGS. Indeed, $\Delta E^{(1)} = E_{\text{RES}} - E_{\text{GTS}} \cong p_1 \hbar\omega_1 = 0.80$ eV, while $\Delta E^{(2)} = E_{\text{GTS}} - E_{\text{URGS}} \cong p_2 \hbar\omega_2 = 1.38$ eV, which summed up give 2.18 eV, almost equal to the emission energy value $E_e = 2.34$ eV. The energies of the phonons involved in the two radiationless transition W_1 and W_2 are $\hbar\omega_1 = 42.3$ meV and $\hbar\omega_2 = 24.7$ meV, of the same order of magnitude as those of the phonon modes in LiF, which vary from 24 to 50 meV.³⁸

VI. CONCLUSIONS

Almost all the experimental results on the optical properties of F_3^+ centers in LiF can be explained by introducing a triplet state. More precisely, only the ground level of the triplet state seems to play a major role in the optical cycle at the wavelengths and pumping powers used in the present experiments. However, we cannot exclude a minor role of an excited level of the triplet state, which could explain a time

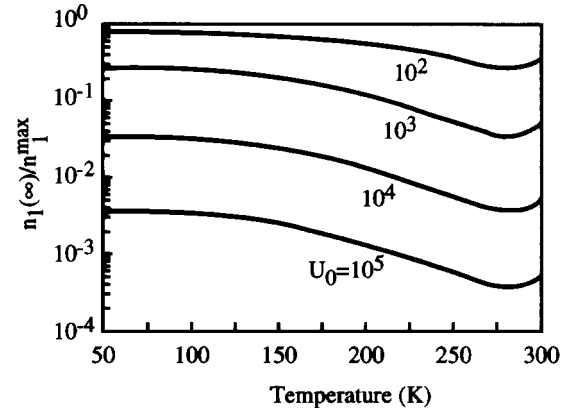


FIG. 14. $n_1(\infty)/n_1^{\text{max}}$ alias the steady-state emission intensity under cw laser pumping, as a function of temperature for different values of the pump rate.

constant of the order of a few μs detected in the present work in emission measurements with a phase-tag technique, a small pump-induced absorption band on the high-energy side of the F_3^+ absorption band,²⁷ and a resonant two-photon absorption at 411 nm.²⁶ We leave the analysis of these details to future investigations, which are necessary for a more complete description of the optical cycle of F_3^+ centers. Indeed there are conflicting interpretations of the most recent non-linear experiments, which result in different energy state layouts for the F_3^+ centers.^{26,27} However our measurements and interpretation have shown that the GTS sits ~ 1 eV below the RES, which is an important result to take into account in any attempt to outline a configuration-coordinate energy diagram.

Moreover the present work has shown that the ground level of the TS can trap a sizeable fraction of the F_3^+ population, which therefore does not participate in the radiative optical cycle. However, because of the temperature variation of W_1 and W_2 , shown in Figs. 12 and 13, this frozen population decreases with decreasing temperature. This effect can be calculated quantitatively by using Eq. (5), the inverse of which gives the steady-state population of the radiative optical cycle, i.e., the emission intensity, under optical pumping. The results, reported in Fig. 14 for different values of U_0 , show that the emission intensity can be one order of magnitude higher at low temperature compared to RT.

It should be also pointed out that the numerical values reported in Fig. 14 depend, among other things, on knowing exactly the lifetime of the RES τ_0 . However, a detailed analysis of previous works has shown that this parameter has not yet been very well determined. Indeed, the values reported in the literature^{28–33} vary from 4 to 12 ns and do not show a clear dependence on temperature,²⁸ while impurities such as Mg and Na seem to affect the values.^{29,30} Moreover, the measurements were carried out for crystals that were poorly characterized as regards the F_3^+ center content, with the exception of the most recent measurement, $\tau_0 = 6$ ns at liquid-helium temperature,³³ which however must be taken with extreme caution. Thus, good lifetime measurements on well-prepared samples are required in order to acquire basic knowledge and to calculate crucial parameters of the optical cycle.

In conclusion, the optical cycle of the F_3^+ center in LiF is

now sufficiently understood, and its basic parameters can be derived in a first approximation and used as in Fig. 14, although other measurements are under way to complete a detailed description. These results show that, apart from a surprising increase of the emission above 270 K, which is useless from a practical point of view because of the thermo-optical instabilities of the F_3^+ center, better conditions for laser action exist at LNT with respect to RT, which in spite of posing additional technical problems is still suitable for

LiF crystals if we take into account their good physical properties.

ACKNOWLEDGMENTS

The authors gratefully acknowledge Dr. T. T. Basiev and L. Bosi for helpful discussions and Dr. E. De Nicola for her contribution in the last stage of the work. Many thanks are also due to A. Pace for his technical assistance.

- *Present address: Pontificia Universidade Catolica do Rio de Janeiro, Departamento de Fisica, Rio de Janeiro, Brazil.
- †Institute of Molecular and Atomic Physics, Academy of Sciences of Belarus, Minsk, Belarus.
- ¹*Physics of Color Centers*, edited by W. B. Fowler (Academy, New York, 1968).
- ²G. Baldacchini, in *Advances in Nonradiative Processes in Solids*, edited by B. Di Bartolo (Plenum, New York, 1991), p. 219.
- ³W. Gellermann, *J. Phys. Chem. Solids* **52**, 249 (1991).
- ⁴Yu. L. Gusev, S. I. Marennikov and S. Yu. Novozhilov, *Kvant. Elektron. (Moscow)* **5**, 1685 (1978) [*Sov. J. Quantum Electron.* **8**, 960 (1978)].
- ⁵V. A. Arkhangel'skaya and P. P. Feofilov, *Kvant. Elektron. (Moscow)* **7**, 1141 (1980) [*Sov. J. Quantum Electron.* **10**, 657 (1980)].
- ⁶T. T. Basiev, S. B. Mirov, and V. V. Osiko, *IEEE J. Quantum Electron.* **QE-24**, 1052 (1988).
- ⁷T. Tsuboi and H. E. Gu, *Appl. Opt.* **33**, 982 (1994).
- ⁸Gu Honggen, *Chin. J. Infrared Millim. Waves* **10**, 7 (1990).
- ⁹T. Tsuboi and H. E. Gu, *Radiat. Eff. Defect Solids* **134**, 349 (1995).
- ¹⁰L. Gomez and S. Morato, *J. Appl. Phys.* **66**, 2754 (1989).
- ¹¹F. De Matteis, M. Leblans, W. Joosen, and D. Schoemaker, *Phys. Rev. B* **45**, 10 377 (1992).
- ¹²L. Bosi, P. Podini, and G. Spinolo, *Phys. Rev.* **175**, 1133 (1968).
- ¹³J. Nahum and D. A. Weigand, *Phys. Rev.* **154**, 817 (1967).
- ¹⁴L. X. Zheng and L. F. Wan, *Opt. Commun.* **55**, 277 (1985).
- ¹⁵A. P. Voitovich, V. S. Kalinov, and I. I. Kalosha, *Dokl. Akad. Nauk BSSR* **30**, 132 (1986).
- ¹⁶A. P. Voitovich, V. S. Kalinov, S. A. Mikhnov, and S. I. Ovseichuk, *Kvant. Elektron. (Moscow)* **14**, 1225 (1987) [*Sov. J. Quantum Electron.* **17**, 780 (1987)].
- ¹⁷A. Meyer and R. F. Wood, *Phys. Rev.* **133A**, 1436 (1964).
- ¹⁸J. Nahum, *Phys. Rev.* **158**, 814 (1967).
- ¹⁹Hong-En Gu, Lan Qi, Liang-Feng Wan, and Hong-Shi Guo, *Opt. Commun.* **70**, 141 (1989).
- ²⁰T. T. Basiev, S. B. Mirov, and V. V. Ter-Mikirtychev, *Proc. SPIE* **1839**, 222 (1991).
- ²¹T. Tsuboi and V. V. Ter-Mikirtychev, *Opt. Commun.* **116**, 389 (1995).
- ²²G. Baldacchini, M. Cremona, G. d'Auria, V. Kalinov, and R. M. Montoreali, *Radiat. Eff. Defect. Solids* **134**, 425 (1995).
- ²³G. Baldacchini, M. Cremona, R. M. Montoreali, L. C. Scavarda do Carmo, R. A. Nunes, S. Paciornik, F. Somma, and V. Kalinov, *Opt. Commun.* **94**, 139 (1992).
- ²⁴S. Paciornik, R. A. Nunes, J. P. von der Weid, L. C. Scavarda do Carmo, and V. S. Kalinov, *J. Phys. D* **24**, 1811 (1991).
- ²⁵M. Cremona, G. Baldacchini, R. M. Montoreali, F. Somma, V. Kalinov, and L. C. Scavarda do Carmo, *Abstracts of the Annual Congress of the National Group of Structure of the Matter* (Monteporzio Catone, Roma, 1991), p. A41.
- ²⁶V. V. Ter-Mikirtychev and T. Tsuboi, *Phys. Status Solidi B* **190**, 347 (1995).
- ²⁷T. T. Basiev, I. V. Ermakov, P. G. Zverev, and V. V. Ter-Mikirtychev, in *Proceedings of the International Conference On Tunable Solid State Lasers, Minsk, Belarus, 1994*, edited by A. P. Voitovich and V. S. Kalinov (Institute of Molecular and Atomic Physics of the Academy Of Sciences of Belarus, Minsk, 1995), p. 68.
- ²⁸L. Bosi, C. Bussolati, and G. Spinolo, *Phys. Lett.* **32A**, 159 (1970).
- ²⁹T. Kurobori, Y. Imai, and N. Takebuchi, *Opt. Commun.* **64**, 259 (1987).
- ³⁰T. Kurobori, T. Kanesaki, Y. Imai, and N. Takebuchi, *J. Phys. C* **21**, L397 (1988).
- ³¹E. Martins, *Tesi di Mestrado* (Universidade de São Paulo, Instituto de Fisica, São Paulo, 1990), p. 85.
- ³²A. G. Bazylev, V. S. Kalinov, S. A. Mikhnov, S. I. Ovseichuk, and L. K. Scavarda do Carmo, *Zh. Prikl. Spektrosk.* **57**, 504 (1992) [*J. Appl. Spectrosc. (USSR)* **57**, 894 (1992)].
- ³³W. von der Osten (private communication).
- ³⁴H. Yu. Gorkov and V. A. Chepurnoi, *Opt. Spektrosk.* **67**, 1088 (1989) [*Opt. Spectrosc. (USSR)* **67**, 642 (1989)].
- ³⁵B. Di Bartolo and R. Peccei, *Phys. Rev.* **137A**, 1770 (1965).
- ³⁶L. A. Riseberg, in *Radiationless Processes*, edited by B. Di Bartolo (Plenum, New York, 1980), p. 369.
- ³⁷U. G. Caldino and J. O. Rubio, *Radiat. Eff. Defect Solids* **127**, 83 (1993).
- ³⁸*Physics of Color Centers* (Ref. 1), p. 267.